Exploiting sparsity in the difference images to achieve higher acceleration factors in non-contrast MRA

P. Storey[1], R. Otazo[1], L. Fleysher[1], N. Oesingmann[2], R. P. Lim[1], V. S. Lee[1], and D. K. Sodickson[1]
[1]Radiology Department, NYU School of Medicine, New York, NY, United States, [2]Siemens Medical Solutions USA

Introduction: It has recently been discovered that patients with renal insufficiency who receive large doses of gadolinium-based contrast agents may be at risk of a rare but serious disorder known as nephrogenic systemic fibrosis (NSF). This has spurred a search for alternatives to conventional first-pass gadolinium-enhanced MRA. Among the methods proposed for non-contrast peripheral MRA are ECG-gated techniques that exploit the pulsatility of arterial blood flow. A flow-sensitive sequence such as FSE [1,2] or diffusion-prepared SSFP [3] is used to acquire two 3D image sets, one in systole when the flow is fast, and one in diastole when the flow is slow. Because of flow-related dephasing, the arteries appear dark on the systolic images, but brighter on the diastolic images, so that subtraction of the systolic images from the diastolic images yields a bright-blood angiogram of the arteries. The need for cardiac gating, however, results in a much longer acquisition time than is required for conventional contrast-enhanced MRA, viz. 2 – 4 minutes per station for non-contrast MRA, depending on heart rate and parameter choices, as compared to 10 – 20 seconds for contrast-enhanced MRA. Long acquisition times increase the probability of subject motion, which compromises the suppression of background tissue in the difference images. Hence there is an interest in finding ways to accelerate the acquisition. Following work by Blaimer and Griswold [4,5] we investigate whether the inherent sparsity of the difference images can be exploited to achieve higher acceleration factors without loss of image quality. To take advantage of the sparsity, subtraction must be performed on the raw data sets before calculation of the GRAPPA weights rather than on the final magnitude images.

Methods: Non-contrast MRA of the calves was conducted on a whole-body 1.5T Siemens Avanto system using a 3D ECG-gated FSE sequence and a peripheral phased array coil. Four healthy subjects (2 men, 2 women) spanning a wide range of ages (26, 35, 51 and 63 years) were included in the study. All provided informed consent. Diastolic and systolic data sets were collected as two measures of a single acquisition with different trigger delays. Diastolic images were acquired with the minimum trigger delay and systolic images with a trigger delay that coincided with peak flow in the popliteal arteries as determined by prior phase contrast imaging. The 3D FSE sequence used non-selective refocusing pulses with a constant flip angle of 100° and echo spacing of 2.82ms, integrated GRAPPA reconstruction with 24 reference lines, and 1–2 echo trains per partition depending on acceleration factor. Other parameters were: FOV=450mm, base resolution=320, slice thickness=1.5mm, phase/slice resolution=92%/75%, TE=79–132ms. Image reconstruction was performed twice for each acquisition, first using the standard reconstruction chain, and second with subtraction of the raw data sets prior to calculation of the GRAPPA kernel. Both reconstructions were performed online using the retrospective reconstruction feature. GRAPPA factors ranging from 2 to 6 were tested, and multiple acquisitions were performed with each to verify consistency and to control for run-to-run variations such as subject motion and heart rate irregularities. Images were presented in randomized order to a board-certified radiologist, who was blinded to the acquisition parameters and reconstruction algorithm. Vessel visualization was graded on a 4-point scale: good/partial/minimal/absent. Separate grades were assigned to large vessels (e.g. popliteal, peroneal and tibial arteries), small vessels (e.g. dorsalis pedis and plantar arteries) and fine branch vessels (e.g. geniculate arteries).

Results: Figs. 1(a–c) show source images obtained using a GRAPPA factor of 2 and a MIP of the difference images. Note that the popliteal artery (arrows) appears dark in systole and brighter in diastole. Note also that the source images are not sparse (although their difference is). Figs. 1(d) and (e) are obtained from an acquisition with a GRAPPA factor of 6, using standard reconstruction (d) and raw data subtraction (e). Note the reduction of pseudo-noise and improved depiction of vessels in (e). A summary of the results for vessel visualization is given in Fig. 2. For large vessels, visualization with GRAPPA 6 and raw subtraction is similar to that for GRAPPA 2. For small and branch vessels, visualization for GRAPPA 6 is greatly improved using raw subtraction, but does not match that obtained with GRAPPA 2.

Discussion: The inherent sparsity of the difference images in non-contrast MRA can be exploited to achieve higher acceleration factors by performing subtraction on the raw data prior to calculation of the GRAPPA weights rather than on the final magnitude images. Using this alternative reconstruction, visualization of large vessels was well preserved up to very high acceleration factors. However visualization of small vessels and fine branch vessels was compromised. This may be due to the least-squares algorithm used in calculation of the GRAPPA kernel, which gives more weight to areas of higher signal. **Acknowledgements:** NIH HL092439, EB000447

References: [1] Miyazaki M, Radiol 2003; 227:890 [2] ISMRM 2008, 730 [3] Fan Z, MRM Oct 2009 [4] ISMRM 2007, 749 [5] ISMRM 2008, 1270

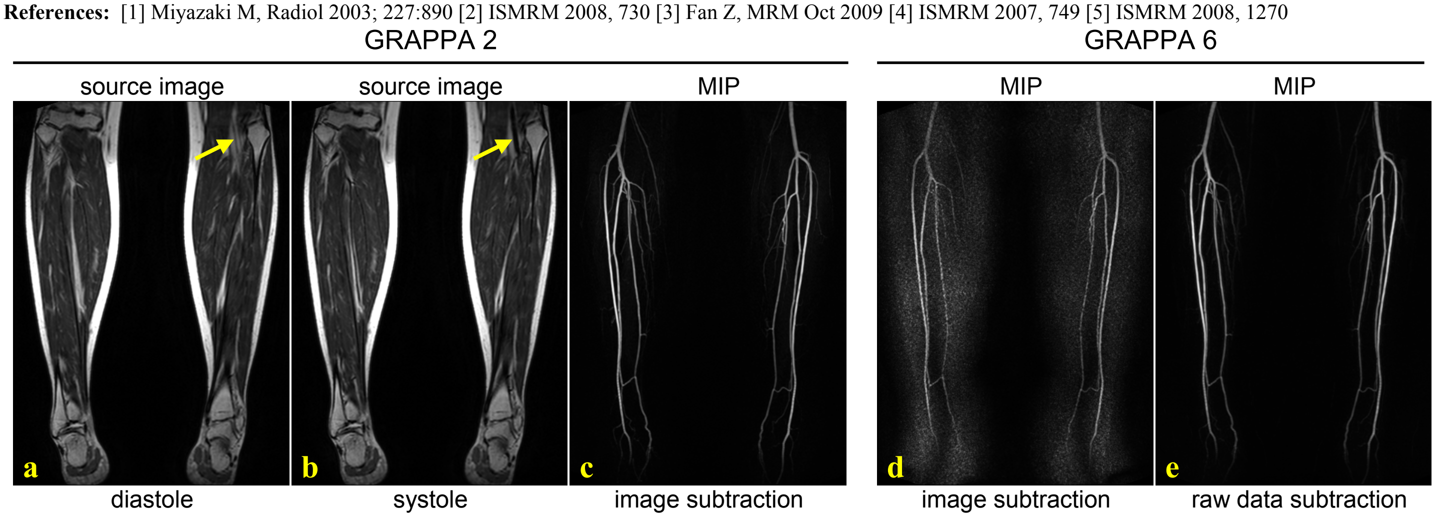

Figure 1: Results in a 35 year old woman. Diastolic (a) and systolic (b) source images from a single slice, and a MIP (c) of the difference images, obtained using an acceleration factor of 2 and standard reconstruction. (d) and (e) are MIPs obtained from an acquisition with an acceleration factor of 6. Standard reconstruction with subtraction of the magnitude images was used in (d), and modified reconstruction with subtraction of the raw data in (e). No image filtering or sculpting was applied.

Figure 2: Vessel visualization in all 4 subjects. Comparison of standard reconstruction ('std recon') with raw data subtraction ('raw sub') is made for 27 data sets acquired with GRAPPA 6. Further comparison is made with 13 data sets acquired with GRAPPA 2. TE was similar for all data sets.